CHAPTER IV
RESULTS AND DISCUSSION

This chapter illustrates the model validation which compares the simulated results with historical data from real reservoir, sensitivity analysis of reservoir parameters such as rock permeability-rock porosity, numerical methods, and simulation results from the based case and realistic case as discussed below.

4.1 Model Validation

In this part, the related equations described in chapter III were solved by the finite difference and finite element method, respectively. The model was tested in many cases including regular and irregular shapes with constant/inconstant permeability after gas withdrawal or injection, and actual reservoir geometry. The model investigated the reservoir behaviors such as pressure distribution, wellbore pressure, bottom well pressure and production time after gas withdrawal/injection with respect to time. Finally, the historical data from the actual reservoir geometry were matched in the model, as shown below.

The carbonate reservoir data from PTT Exploration and Production Public Company Ltd. shown in Figure 3.1(c) and Tables 4.1 and 4.2 contain the geological data of reservoir (shape and size), locations of withdrawal wells and operating condition of reservoir. The model predicted the average reservoir pressure after gas withdrawal at 12 wells. The simulation results from these two numerical methods were plotted with the cumulative withdrawal gas compared to the historical data (PTT Exploration and Production Public Company Ltd.) as shown in Figure 4.1. It is shown that FEM predicted the reservoir pressure close to historical data, while the result from FDM was farther from historical data when cumulative gas increased, because the FEM has the advantage that it can simulate any shape of reservoir better than FDM at the same amount of grid blocks and elements. Then, the accuracy of FEM approximation is higher than in the corresponding FDM approach.

Table 4.1 Location of withdrawal wells (PTT Exploration and Production Public Company Ltd.)

Number of wells	Well location (x ft, y ft)
1	(9514 , 12664)
2	(7841 , 10039)
3	(9514 , 7414)
4	(12303 , 5840)
5	(15092 , 7939)
6	(14534 , 10564)
7	(14534 , 17388)
8	(16207 , 19488)
9	(15092 , 22638)
10	(12303 , 22113)
11	(10072 , 22113)
12	(9514 , 20013)

Table 4.2 List of operating condition and input parameters of carbonate reservoir (PTT Exploration and Production Public Company Ltd.)

Item (unit)	Symbol	Value
Operating condition:		
Gas withdrawal rate per well (MMSCFD)	Q_w	80
Reservoir pressure (psi)	p_{re}	2550
Reservoir temperature (R)	T_{re}	599
Properties of gas reservoir:		
Fanning friction factor	f_F	0.0054
Gas Viscosity (cP)	μ	0.0155
Permeability (md)	k	240
Porosity	ε	0.28

Table 4.2 (Cont'd.)

Item (unit)	Symbol	Value
Reservoir geometry:		
Reservoir length (ft)	L	32,152
Reservoir thickness (ft)	H	333
Reservoir width (ft)*	W	24,935
Well depth (ft)	wd	4166
Well radius (ft)	r_w	0.3

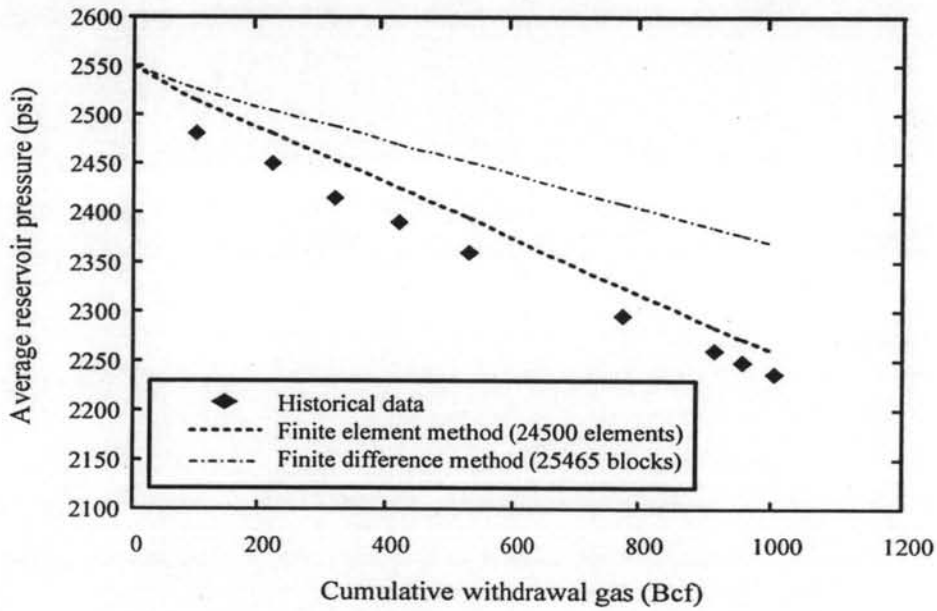

Figure 4.1 Relationship between cumulative withdrawal gas and average reservoir pressure.

4.2 Sensitivity Analysis

The sensitivity analysis is aimed at studying the effect of reservoir parameters obtained from finite different and finite element methods. The reservoir geometry considered here is in regular shape as mentioned earlier in Section 3.1. The input data is indicated in Table 4.3. The effect of grid subdivision in the FDM is determined. The reservoir life time and operated pressure were compared by these

two numerical methods. Moreover, the effects of rock permeability and rock porosity on the well pressure inside the reservoir were investigated.

Table 4.3 List of operating condition and input parameters of regular and irregular shape reservoirs

Item (unit)	Symbol	Value
Operating condition:		
Gas injection rate (MMSCFD)	Q_{in}	3
Gas withdrawal rate (MMSCFD)	Q_w	5
Reservoir pressure (psi)	p_{re}	1000
Reservoir temperature (R)	T_{re}	560
Production time (days)	T	500
Properties of gas reservoir:		
Fanning friction factor	f_F	0.0047
Gas Viscosity (cP)	μ	0.05
Permeability (md)	k	100
Porosity	ε	0.148
Reservoir geometry:		
Reservoir length (ft)	L	5000
Reservoir thickness (ft)	H	50
Reservoir width (ft)	W	5000
Well depth (ft)	wd	4000
Well radius (ft)	r_w	0.5

4.2.1 Effect of Grid Subdivision

This part aimed to find the optimum blocks in FDM that perform the accurate results. The idea is that if further refinement shows no change in the results, then the results are accurate and no additional refinement is needed. The regular case is used to study this effect based on the data from Table 4.3. The location of well is

assumed at center of reservoir (2500, 2500 ft) for neglecting the boundary effect. A number of locations represent the investigated points around the well as shown in Figure 4.2. The distance of each point equals 1000 ft.

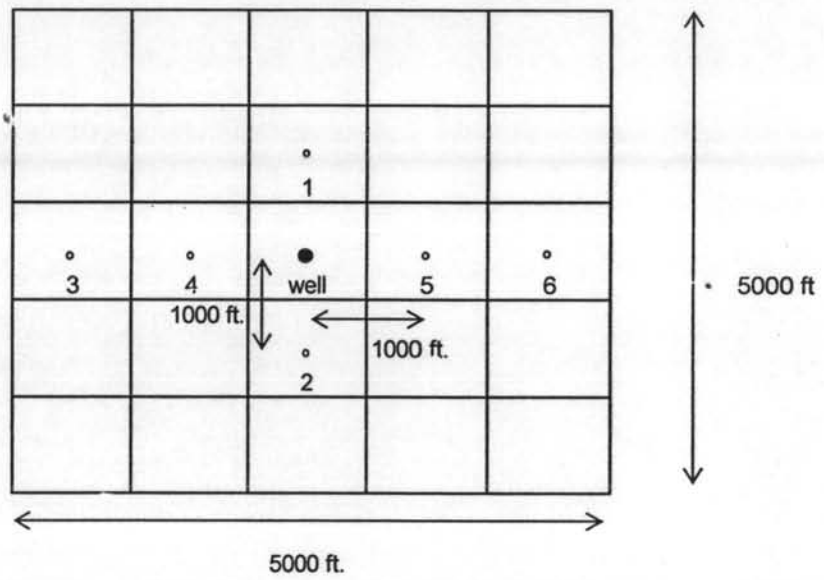

Figure 4.2 Location of investigated point.

The relation between pressure at investigated points around the well and total blocks is shown in Table 4.4. It is observed that the well is located at the center of reservoir. The pressures in each total blocks at investigated points (1, 2, 4 and 5) was similar. When look at the farther blocks (number 3, 6), the pressure was very little change during proceeding from 100 x 100 to 110 x 110 blocks. While the pressures at other points closer to the center were little change too. Therefore, the total blocks equal 10000 (100*100 blocks per axis) blocks were used in this studied.

Table 4.4 Relationship between pressure on investigated points at 500 days and amount of blocks

LOCATION	TOTAL BLOCKS									
	400	900	1600	2500	3600	4900	6400	8100	10000	12100
1	892.77	891.54	890.59	889.77	889.05	888.42	887.86	887.36	886.91	886.5
2	892.65	891.54	890.61	889.79	889.08	888.45	887.89	387.39	886.94	886.53
3	869.8	891.05	897.59	899.29	899.45	899.13	898.69	898.26	897.85	897.77
4	891.6	890.95	890.05	889.27	888.59	887.98	887.45	886.97	886.54	886.15
5	892.14	890.96	890.05	889.27	888.59	887.98	887.45	886.97	886.54	886.15
6	903.29	902.21	901.31	900.53	899.86	899.26	898.74	898.27	897.85	897.77
% alteration	-	0.495	0.207	0.106	0.068	0.064	0.059	0.054	0.048	0.033

** the percentage of alteration = ((pressure at previous blocks – pressure at present blocks)/ pressure at present blocks)*100

4.2.2 Effect of Calculation Methods

The simulation results discussed in this section is aimed at comparing the reservoir and operating conditions obtained from finite difference and finite element methods. The average reservoir pressure, tophole pressure, well pressure, cumulative production gas and reservoir life time are summarized in Table 4.5. From the reservoir pressure compared with historical data in previous section, the accuracy from finite element method was emphasized in this section. It is observed that the results from finite difference method are larger than ones from finite element method because finite difference method has some disadvantage, particularly, sizing of grid scale and reservoir shape.

Table 4.5 Simulated operating results

Conditions	Numerical Methods	
	FDM	**FEM**
Tophole pressure (psi) at 500 days	649.81	614.86
Well pressure (psi) at 500 days	699.78	662.15
Cumulative production gas (BCF) at minimum delivery pressure, 400 psi	7.35	6.35
Reservoir life time at minimum delivery pressure, 400 psi (days)	1470	1270

4.2.3 Effect of Rock Porosity and Permeability

In order to constitute a commercial hydrocarbon reservoir, there are two basic requirements for a reservoir, i.e., rock porosity and rock permeability. Porosity, representing the capacity of gas storage, is defined as a percentage or fraction of void relative to the bulk volume of a rock. Permeability is a qualitative measurement of porous material that permits the movement of fluid under a pressure gradient, typically measured in millidarcy (md). The permeability – porosity relationship has always considered as a very valuable tool for interpreting petrophysical properties of the rock. In general, permeability is a function of rock

porosity, grain size and packing arrangement (size and shape of the pores), pore connectivity and orientation, capillary structure, as well as cementation and the rock's depth. In this work, the correlation to calculate the permeability using porosity for carbonate reservoirs was used as indicated below (Sadooni, 2002).

$$k = 126.7\varepsilon R_p^{\,2} \tag{4-1}$$

where, R_p is the pore radius in reservoir rock (microns).

The average porosity of a reservoir rock generally range from 10 to 40 % and pore-throat diameters between 0.5 and 5 microns (mesopores). The rock porosity in this study is in the range of 10 to 40%. The permeability versus porosity at 2.5 microns of pore radius is illustrated in Figure 4.3. The well pressure after gas withdrawal is shown in Figure 4.4. It is observed that low porous reservoir (low permeability) that contains small amount of gas should be operated at lower well pressure (high pressure gradient) than high porous reservoir at the same production gas. This can be explained by the Darcy's Law that the pressure gradient is inversely proportional to the permeability. As a result, the porosity - permeability of rock have effect to the reservoir life time.

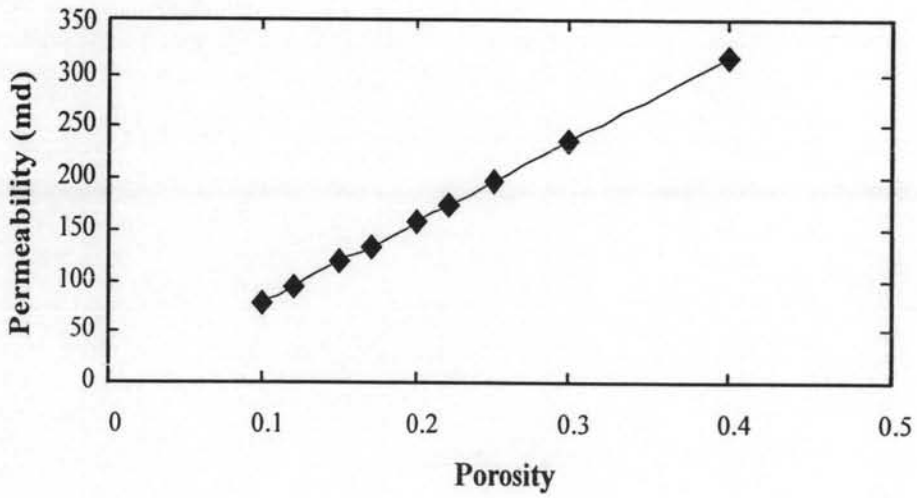

Figure 4.3 Relationship between permeability and porosity.

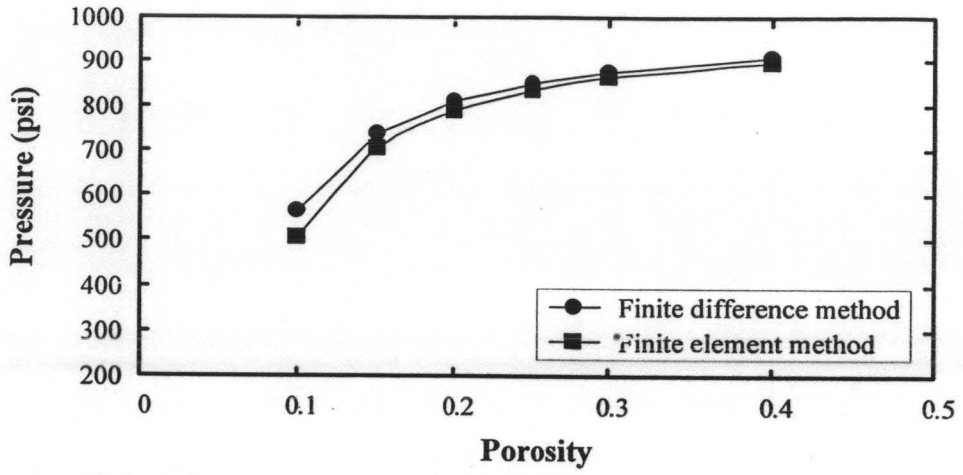

Figure 4.4 Relationship between well pressure and rock porosity.

4.3 Simulation Results

The simulation results discussed in this section is aimed at comparing the pressure profiles obtained from finite different and finite element methods. The reservoir geometries considered here are in regular, irregular and carbonate shapes as mentioned earlier in Section 3.1. For regular and irregular shapes, the effect of inconstant permeability on the pressure profile inside the reservoir was also investigated. The based case input data of regular and irregular shape reservoirs is summarized in Tables 4.3 while those of carbonate reservoir are already indicated in Table 4.2.

4.3.1 Regular Shape Reservoir

4.3.1.1 Constant Permeability

The pressure profiles after gas withdrawal at (1750, 1750 ft) for 500 days using finite difference and finite element methods are shown in Figures 4.5(a) and (b), respectively. The amount of elements in Figures 4.5(a) and (b) are 10000 and 10200 elements, respectively. FDM spent approximately 4 minutes to compute the pressure profile which is less than that calculated by FEM about 2 minutes. It is observed that pressure profile dramatically decreases at the vicinity of

the bottom well. This can be explained by the fact that the pressure gradient ($p_r > p_w$) around the bottom well causes natural gas flowing toward the bottom well.

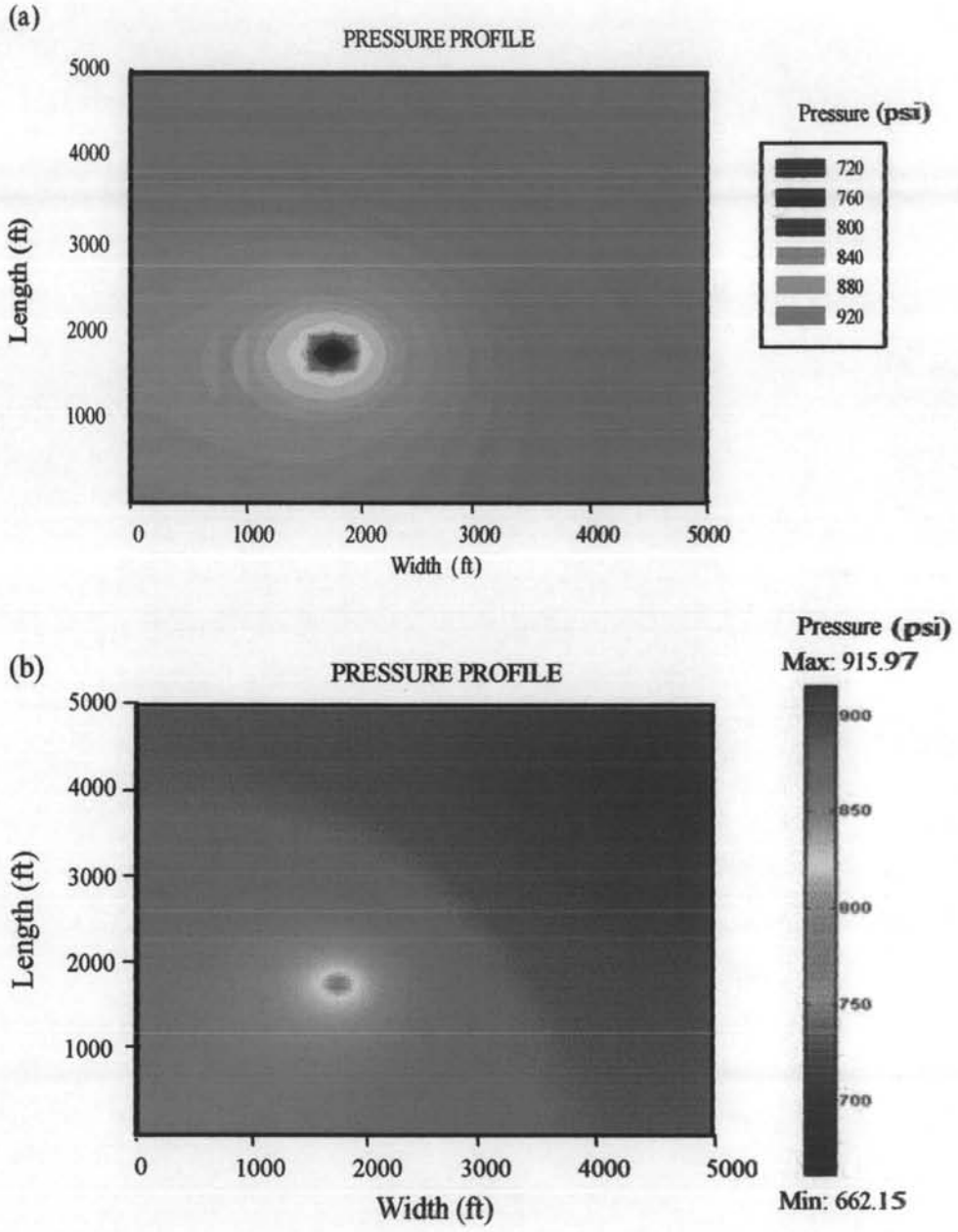

Figure 4.5 Pressure profiles after withdrawal gas at time 500 days, (a) finite difference method, (b) finite element method.

The pressure profile after gas withdrawal at (1750, 3500 ft) and injection at (3500, 1750 ft) is illustrated in Figures 4.6(a) and (b). The pressure profile obtained from finite different method (Figure 4.6(a)) is similar to that achieved from finite element method (Figure 4.6(b)). The pressure profile shown in this figure indicate that, at the injection point, the bottom well pressure is higher than reservoir pressure ($p_w > p_r$) because natural gas flows downward into reservoir. On the contrary, the reservoir pressure must higher than the bottom well pressure at withdrawal point as previously mentioned. As a result, the reservoir pressure gradually decreases at withdrawal point and increases at injection point.

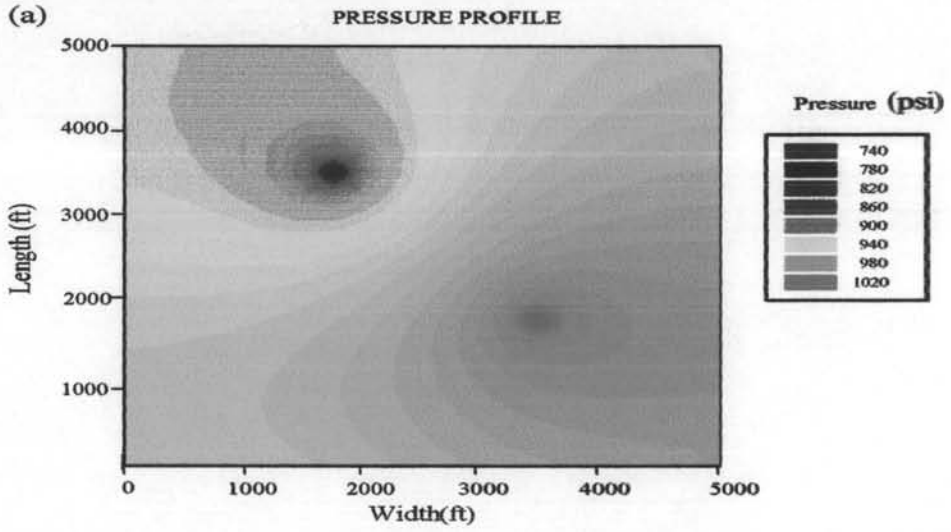

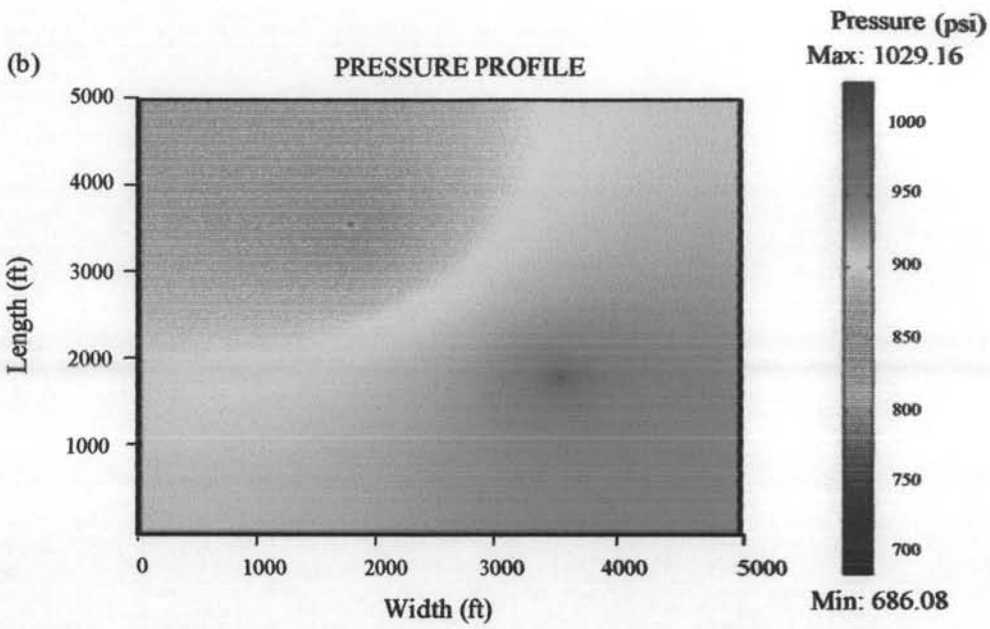

Figure 4.6 Pressure profiles after withdrawal / injection gas at time 500 days, (a) finite difference method, (b) finite element method.

4.3.1.2 Inconstant Permeability

Inherently, the reservoir may contain different kinds of porous rocks causing inconstant permeability. Therefore, the permeability factor is varied relying on location within the reservoir. The permeabilities in this study are in the range of 80 to 140 md as indicated in Figure 4.7, while the overall porosity still constant.

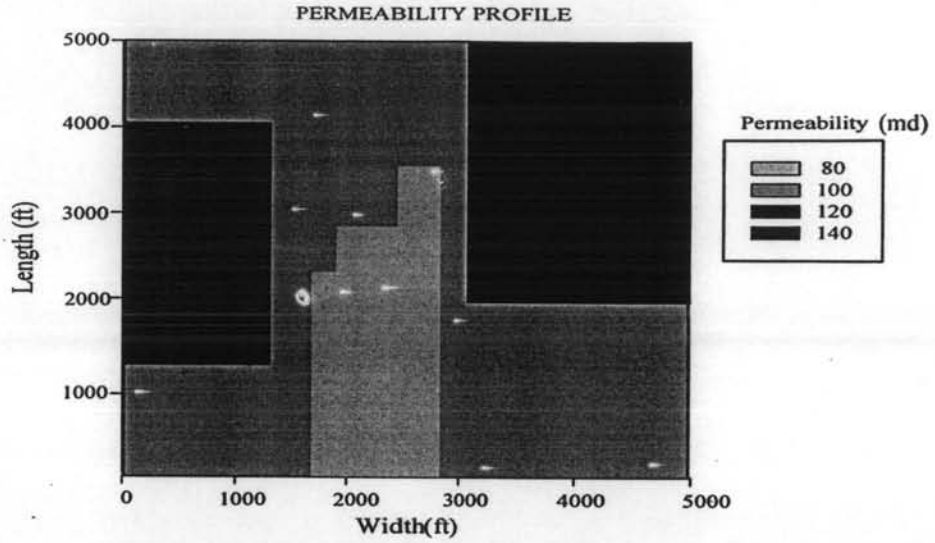

Figure 4.7 Permeability profile in reservoir.

The pressure profile after gas withdrawal at (1750, 1750 ft) in low permeation area (80 md) is shown in Figures 4.8(a) and (b). Comparing this figure to Figure 4.5 where the well is located in high permeation area (100 md). It is observed that the withdrawal well which locates in low permeable area must operates at low bottom well pressure to maintain the same flow rate. This can be explained by the fact that the permeability is inversely proportional to the pressure gradient.

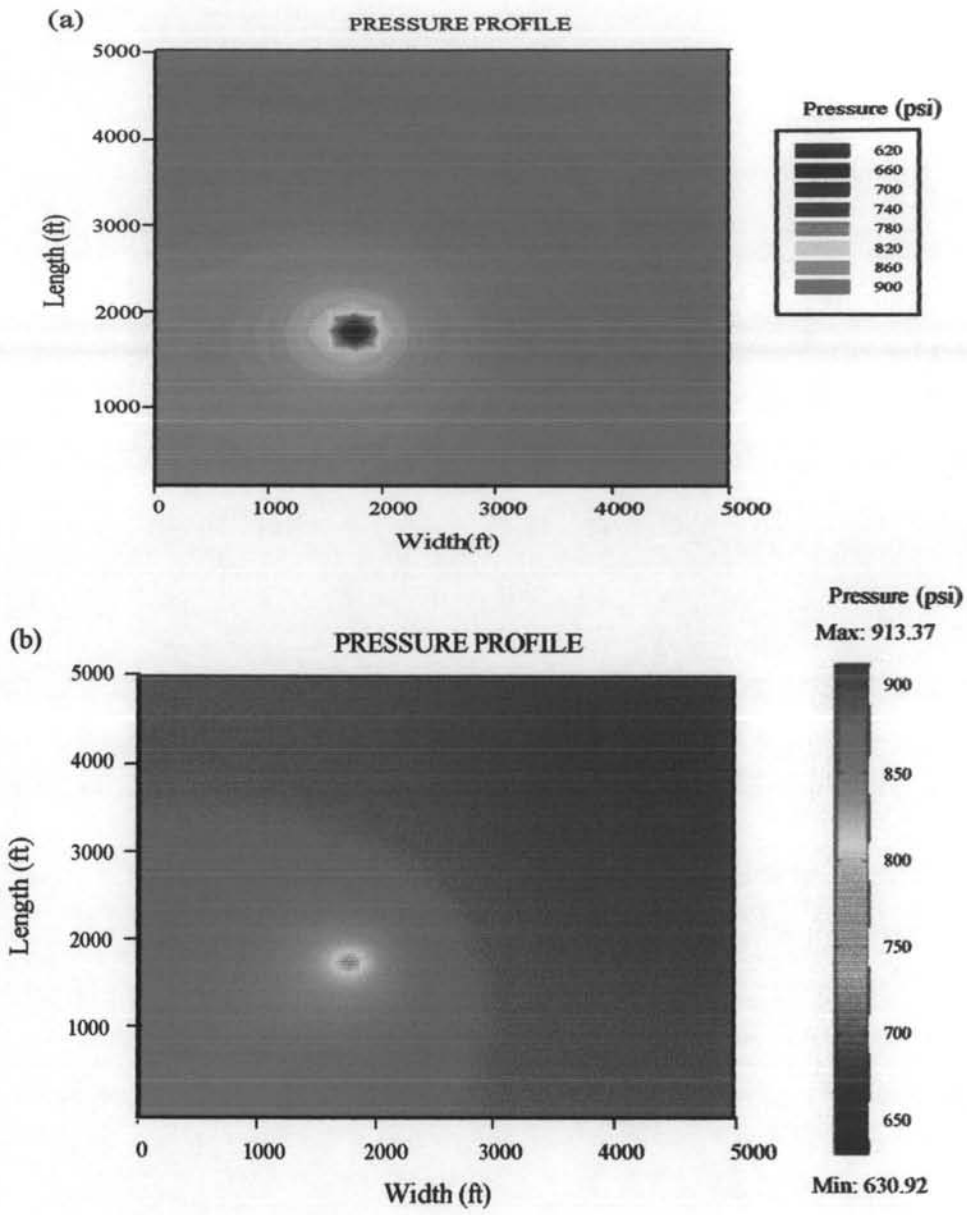

Figure 4.8 Pressure profiles after withdrawal gas in low permeation area (80 md) at time 500 days, (a) finite difference method, (b) finite element method.

The pressure profile after the gas withdrawal at grid point (4000, 3500 ft) in high permeable area (140 md) is depicted in Figures 4.9(a) and (b). It is observed that the bottom well pressure in this case is higher than that of well located in low permeation area under the same withdrawal flow rate.

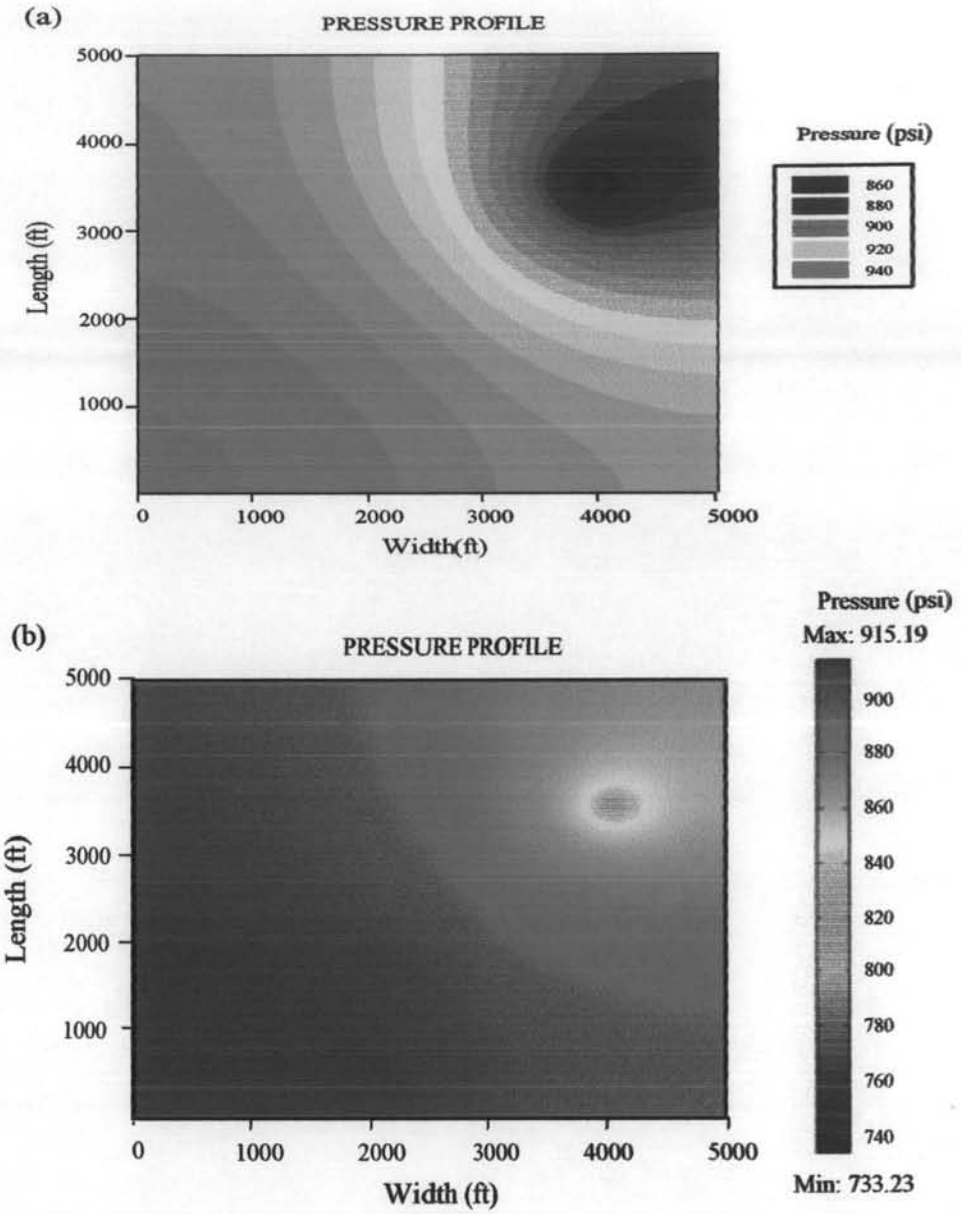

Figure 4.9 Pressure profiles after withdrawal gas in high permeation area (140 md) at time 500 days, (a) finite difference method, (b) finite element method.

The pressure profile after gas withdrawal at (4000, 3500 ft) and injection at (1750, 1750 ft) is shown in Figures 4.10(a) and (b). In this case, the gas is injected in low permeation area (80 md) to push the production gas into the withdrawal point locating in high permeation area (140 md). As a result, the withdrawal point is operated at higher bottom well pressure than the previous case (Figure 4.9).

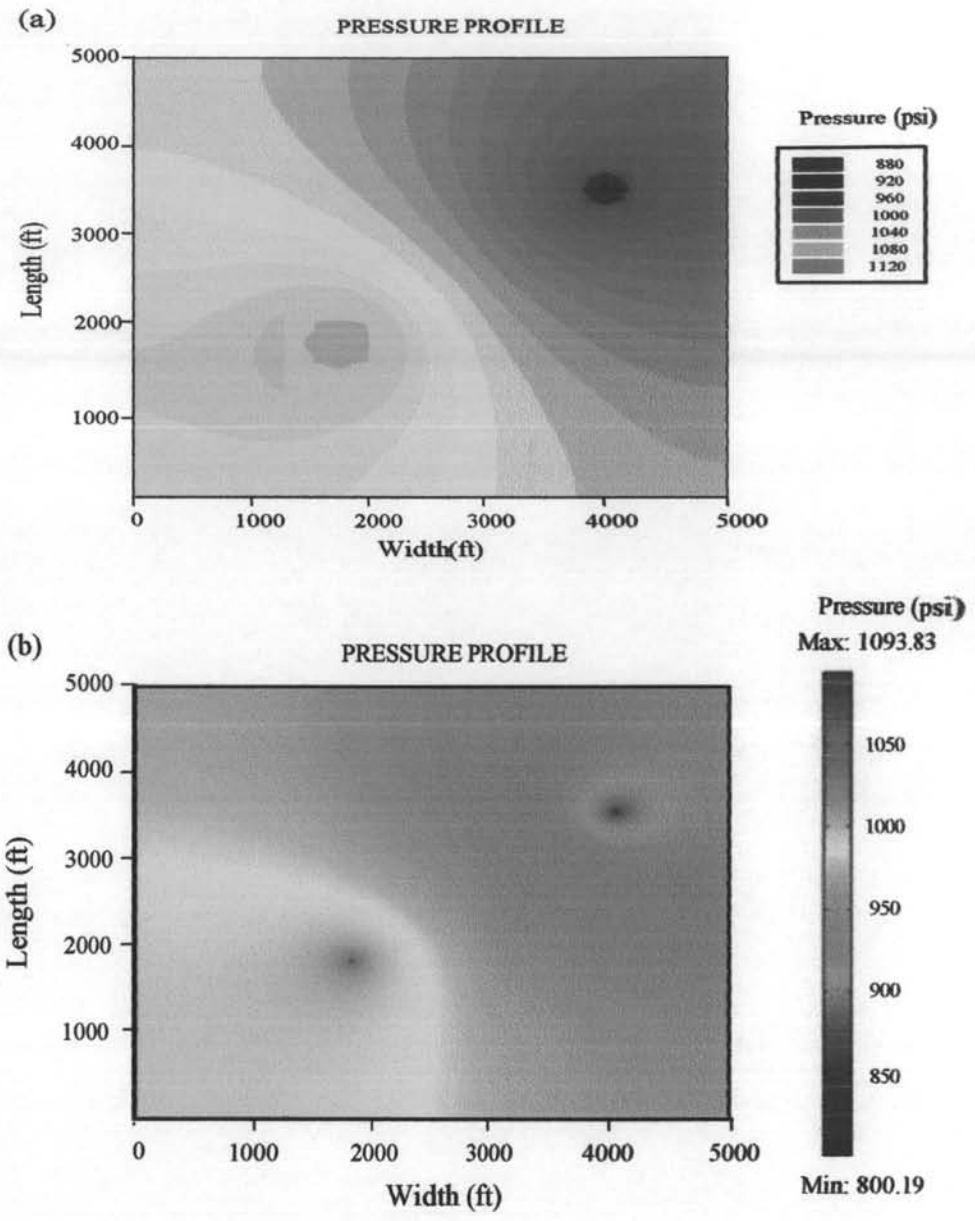

Figure 4.10 Pressure profiles after gas withdrawal and injection at time 500 days, (a) finite difference method, (b) finite element method.

4.3.2 Irregular Shape Reservoir

Since the actual reservoir geometry does not form the rectangular shape, the curved edge and interior islands must be considered in this model development as previously discussed in Section 3.1.

4.3.2.1 Constant Permeability

The reservoir shape and permeability profile are shown in Figure 4.11.

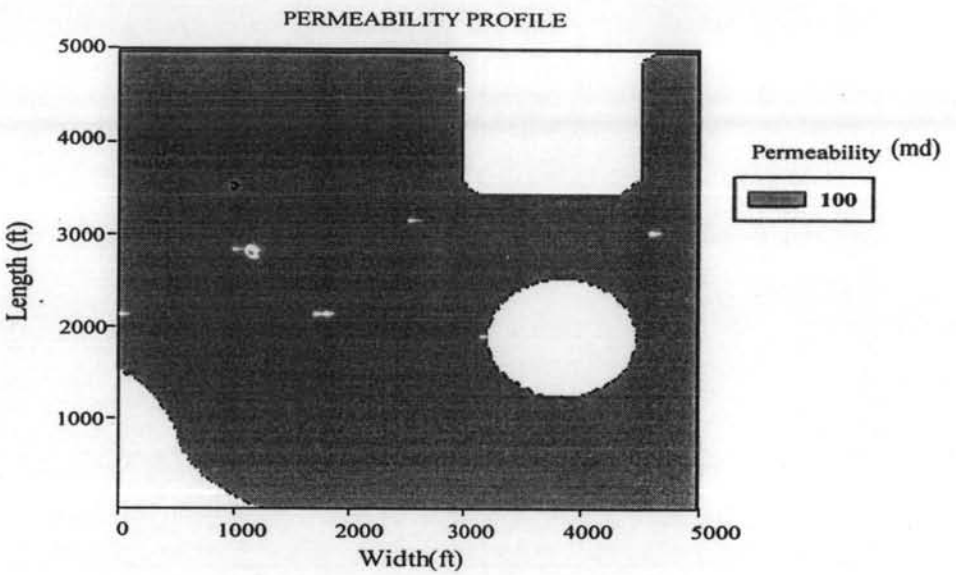

Figure 4.11 Permeability profile in irregular shape reservoir.

The pressure profile after the gas withdrawal at (1000, 3500 ft) is depicted in Figures 4.12(a) and (b). The amount of elements in Figures 4.12(a) and (b) are 8225 and 8382 elements, respectively. The reservoir shape drawn by FEMLAB software (Figure 4.12(b)) is able to represent the actual reservoir rather than that drawn by finite difference method (Figure 4.12(a)). Moreover, the FEMLAB software also presents the direction of gas flow in this model. The gas flows from the niche into the well. It is observed that reservoir pressure gradually decreases at the niche to the well.

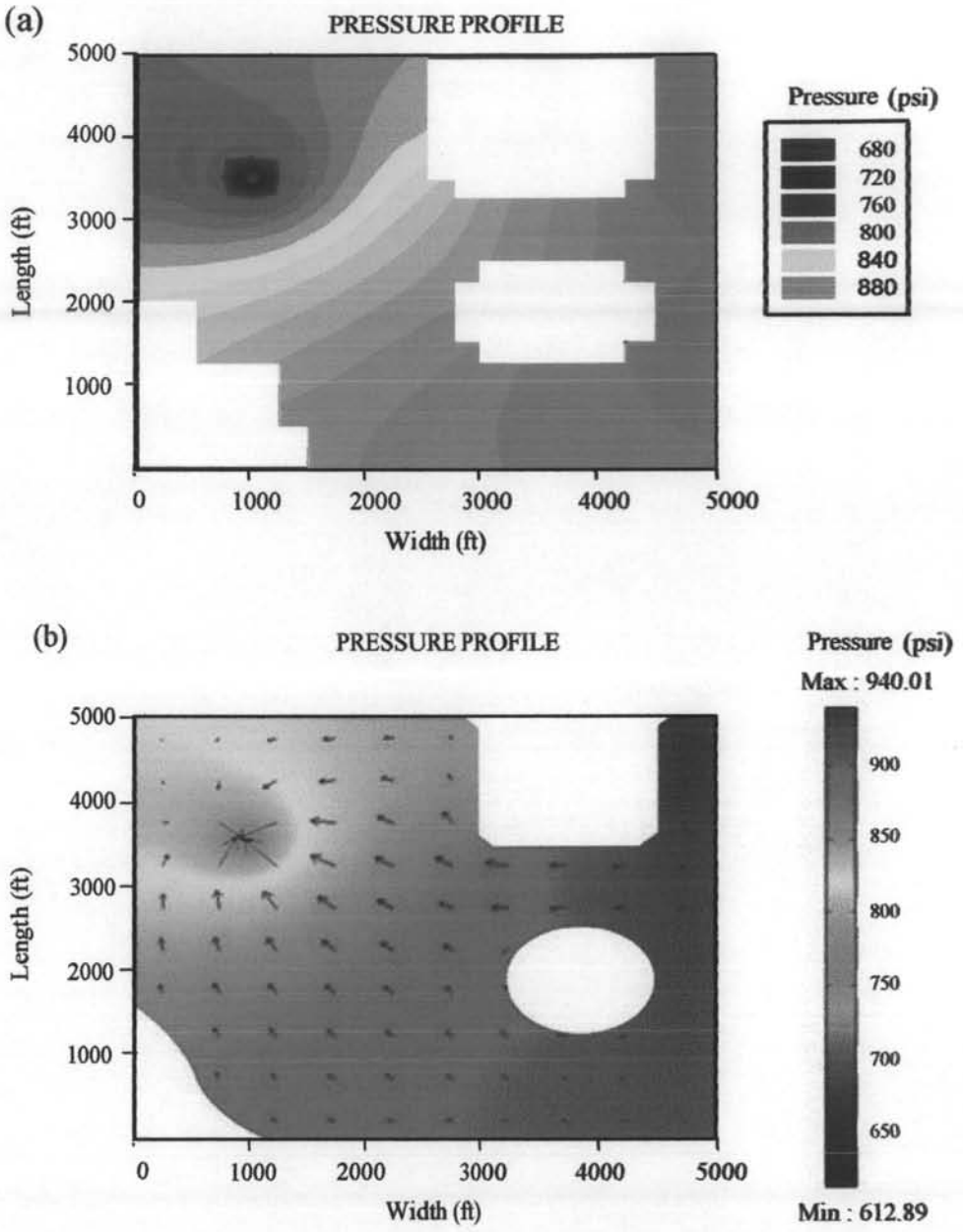

Figure 4.12 Pressure profiles after withdrawal gas in irregular shape reservoir at time 500 days, (a) finite difference method, (b) finite element method.

The pressure profile after gas withdrawal at (1000, 3500 ft) and injection at (4250, 500 ft) is depicted in Figures 4.13(a) and (b). From the direction of gas flow (Figure 4.13(b)), the gas flows from the injection well into the

withdrawal well. As a result, the reservoir pressure gradually decreases at withdrawal point and increases at injection point.

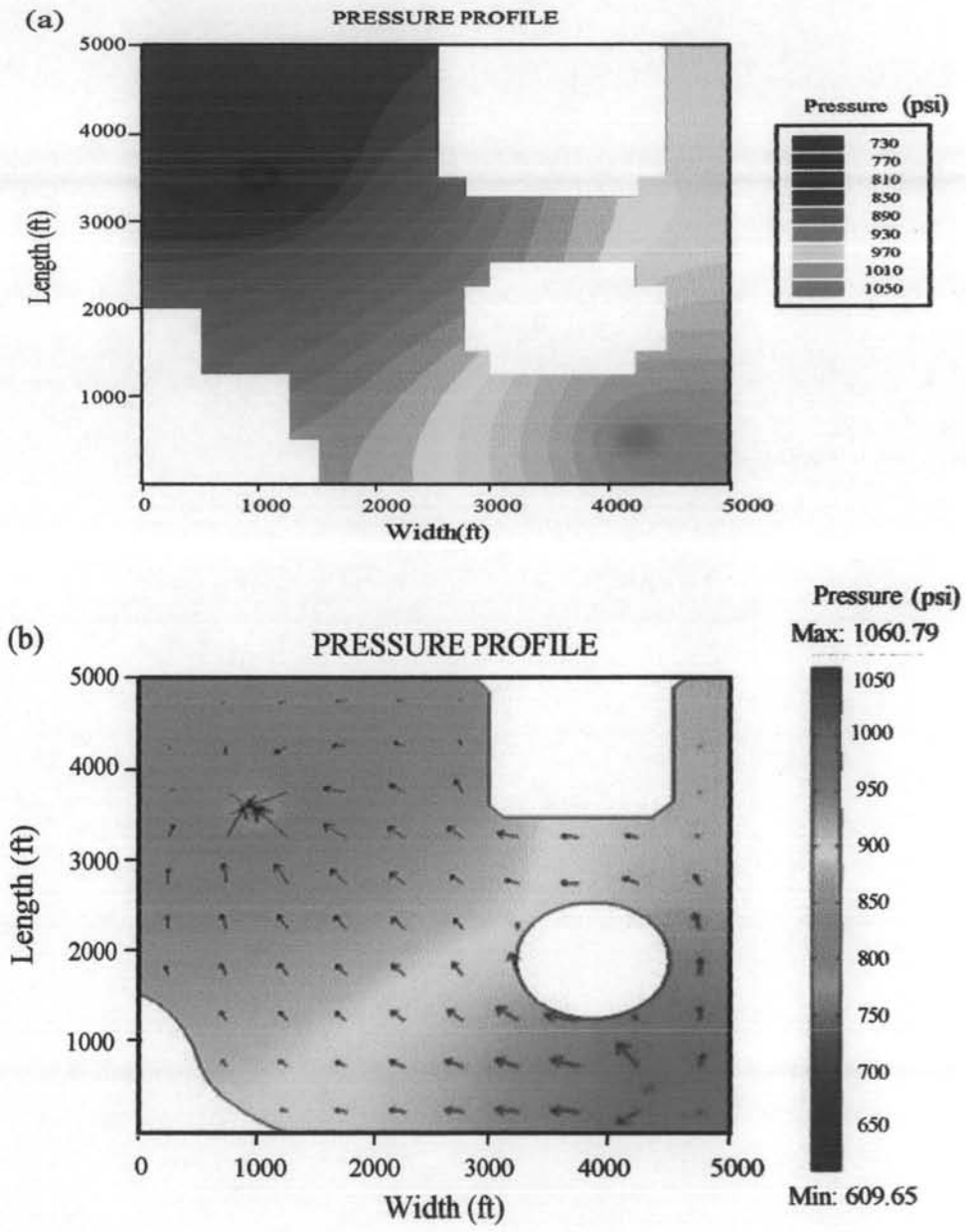

Figure 4.13 Pressure profiles after withdrawal / injection gas in irregular shape reservoir at time 500 days, (a) finite difference method, (b) finite element method.

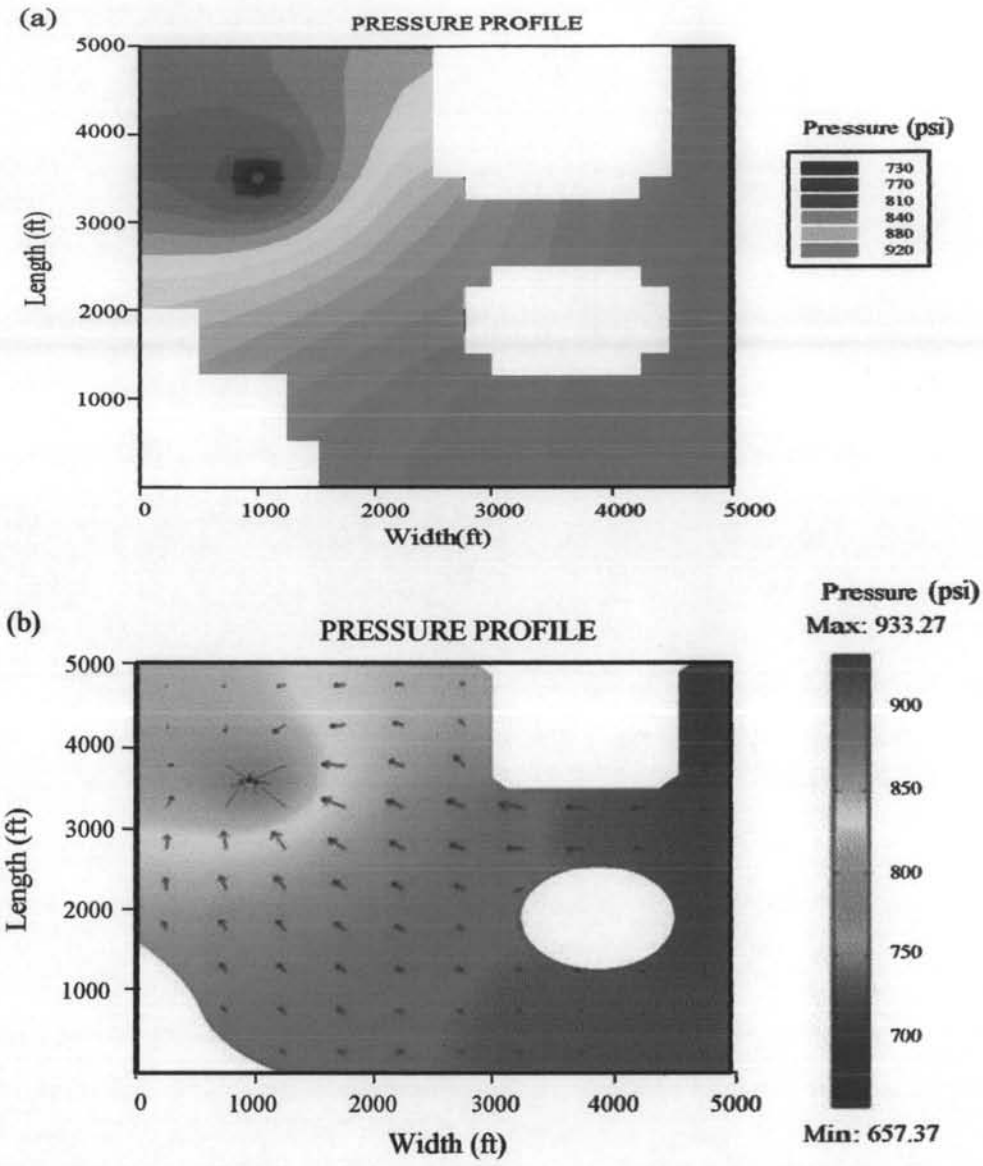

Figure 4.15 Pressure profiles after withdrawal gas in varied permeability reservoir at time 500 days, (a) finite difference method, (b) finite element method.

4.3.3 Realistic case

The simulation results discussed in this section is aimed at applying the model with the realistic situations. First, in case of fluctuation demand, the operation period is divided into 3 zones, i.e., 4 months for withdrawal, 6 months for injection and 2 months for shut in (no operation). The reservoir geometry considered here is in regular. The base case input data is summarized in Tables 4.3. Another is Carbonate reservoir. The actual reservoir data from PTT Exploration and Production

4.3.2.2 Inconstant Permeability

The permeabilities are varied in the range of 80 to 140 md as indicated in Figure 4.14.

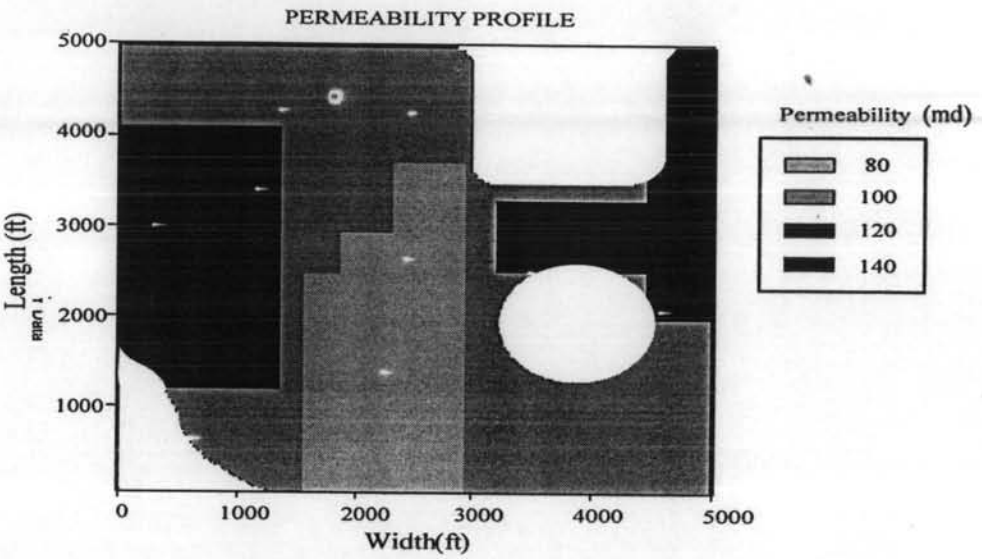

Figure 4.14 Permeability profile of irregular shape reservoir.

The pressure profile after gas withdrawal at (1000, 3500 ft) in high permeation area (120 md) is illustrated in Figures 4.15(a) and (b). Comparing this figure to Figure 4.12 where the well is located in low permeation area (100 md). It is observed that the withdrawal point which locates in high permeable area must operates at high bottom well pressure to maintain the same flow rate.

Public Company Ltd. is used. The simulation results are compared with the historical data which compares between average reservoir pressure and cumulative production gas as discuss in section 4.1.

4.3.3.1 Fluctuation Demand

In the United States, the excess gas pumped during the summer is stored in underground porous-rock formations because the consumer demand for the gas fluctuates substantially from a low point during the summer to a maximum during the winter. This situation was studied in simulation program. The operation period was divided into 3 zones, i.e., 4 months for withdrawal, 6 months for injection and 2 months for shut-in (no operation), as shown in Figure 4.16. The total withdrawal / injection rate depended on operational time and equaled 10 and 8 MMSCFD, respectively. The volumetric flow rate at each simulation time is calculated by Eq. (4-2).

$$Q = Q_{max}\left(1 - \left|\frac{2t}{t_{max}} - 1\right|\right) \qquad (4\text{-}2)$$

when, Q_{max} is maximum volumetric flow rate, Q volumetric flow rate at each time, t_{max} the operation period ,t simulation time.

The pressure profile during operation at (1750, 1750 ft) and (3500, 3500 ft) are illustrated in Figures 4.17(a)-(c). The pressure profile indicate that, at the withdrawal point, the bottom well pressure is lower than reservoir pressure $(p_r > p_w)$ because natural gas flows upward from reservoir. On the contrary, the bottom well pressure must higher than the reservoir pressure at injection point as previously mentioned. As a result, the reservoir pressure gradually decreases during withdrawal period, increases during injection period and steady during shut-in period.

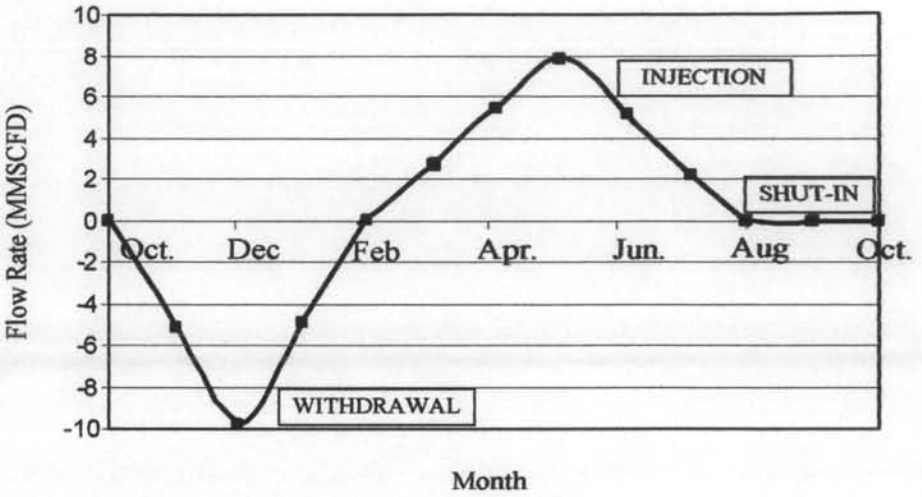

Figure 4.16 Relationship between flow rate and operation time.

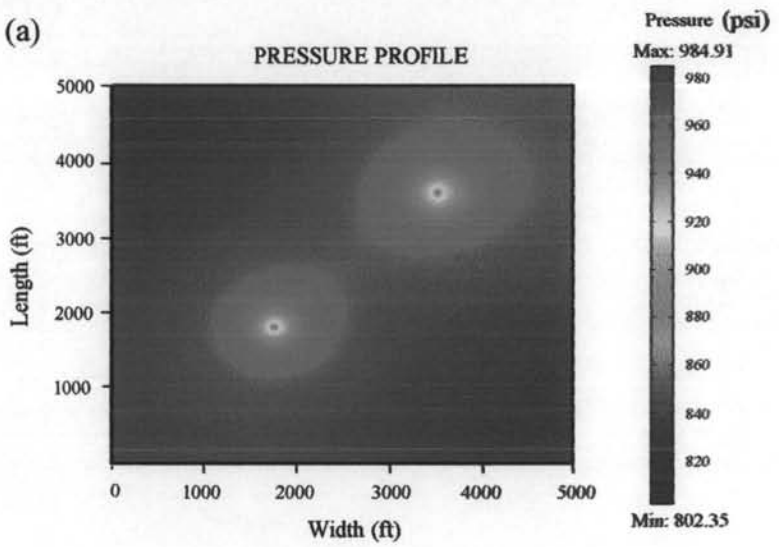

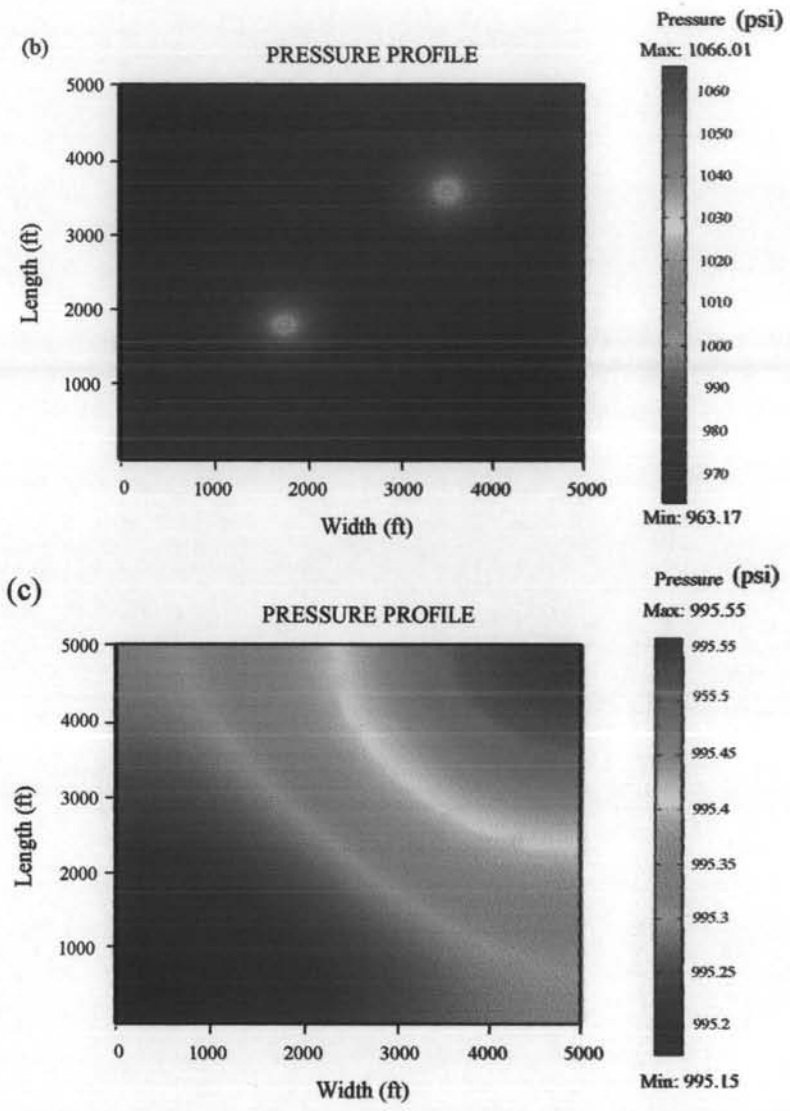

Figure 4.17 Pressure profiles during operation, (a) withdrawal period in December , (b) injection period in May, (c) shut-in period in September.

4.3.3.2 Carbonate Reservoir

In this part, the actual reservoir data from the petroleum company is used to test the numerical method, the finite difference and finite element method, respectively. The model can investigate the reservoir behaviors such as pressure distribution, wellbore pressure, bottom well pressure and production time with respect to time. Furthermore, the simulation results are compared with the

historical data which compares between average reservoir pressure and cumulative production gas as discuss in section 4.1.

The Carbonate reservoir data (Figure 3.1(c) and Tables 4.1 and 4.2) is tested in the model. The reservoir shape and permeability profile are shown in Figure 4.18.

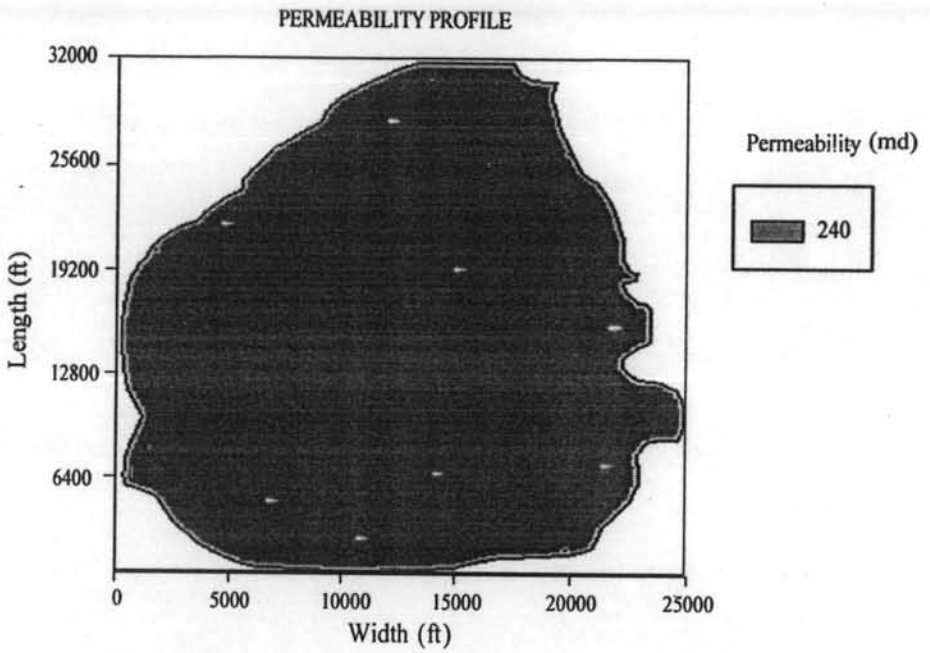

Figure 4.18 Permeability profile of carbonate reservoir.

The pressure profile after gas withdrawal (Q = 80 MMSCFD/well) at 12 wells is shown in Figures 4.19(a) and (b). The amount of elements in Figures 4.19(a) and (b) are 25465 and 24500 elements, respectively. The computation time of pressure profile by FDM (8 minutes) is lower than that by FEM (11 minutes). The reservoir pressure is observed at midpoint, (12303, 10039 ft.) and (12303, 20013 ft.), of carbonate reservoir. At the withdrawal point, the bottom well pressure is less than reservoir pressure (Pr > Pw) that the natural gas flows upward from reservoir to the platform. Consecutively, the reservoir pressure slightly decreases from initial pressure (2550 psi) to the bottom well pressure with respect to time.

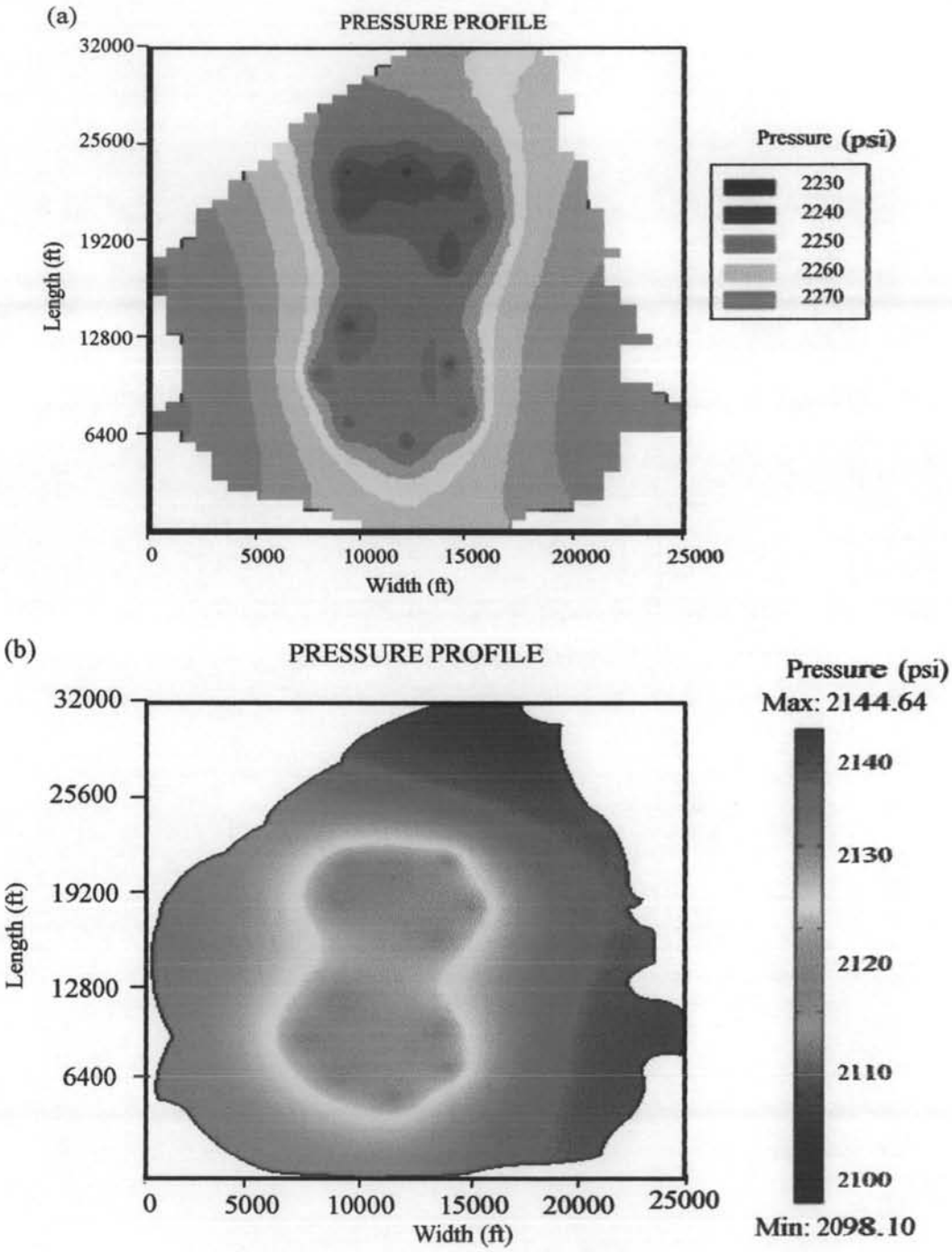

Figure 4.19 Pressure profiles after withdrawal gas in carbonate reservoir at time 5 years, (a) finite difference method, (b) finite element method.